Chinese Chemical Letters 31 (2020) 1978–1981

Contents lists available at ScienceDirect

Chinese Chemical Letters

journal homepage: www.elsevier.com/locate/cclet

Communication

Mechanochemically sulfured $FeS_{1.92}$ as stable and efficient heterogeneous Fenton catalyst

Chao Guo, Dongting Yue, Songling Wang, Xufang Qian, Yixin Zhao*

School of Environmental Science and Engineering, Shanghai Jiao Tong University, Shanghai 200242, China

ARTICLE INFO

Article history:
Received 7 November 2019
Received in revised form 13 November 2019
Accepted 28 November 2019
Available online 29 November 2019

Keywords:
Mechanochemical
Ball milling
Sulfured mackinawite
Heterogeneous Fenton catalysts
Hydroxyl radicals

ABSTRACT

Fenton reaction is one of most promising approaches for efficient removal of various robust organic pollutants in wastewater, however it faces several intrinsic challenges such as acidic condition, sludge waste and sensitive to sulfide-containing compound. Here we reported a novel $FeS_{1.92}$ as an efficient and sulfide resistant heterogeneous Fenton catalyst under mild condition. This novel $FeS_{1.92}$ was facilely prepared through a mechanochemical synthesis of mackinawite (FeS) with sulfur powder (S) by ball milling. The sulfured mackinawite ($FeS_{1.92}$) exhibits high performance in activating H_2O_2 to generate hydroxyle radicals for organic waste remediation. Furthermore, this $FeS_{1.92}$ based heterogeneous Fenton catalyst is highly sulfide resistant and shows improved performance for degrading sulfide-containing organic pollutants. This study provides an effective mechanochemical approach to fabricate heterogeneous Fenton catalysts for sulfide-containing wastewater treatment.

Persistent organic pollutant wastewater remediation has been of vital significance for realizing a sustainable environmental remediation and natural water resource conservation [1–4]. Among various physical and chemical water treatment techniques dealing with organic pollutants in wastewater, advanced oxidation processes (AOPs) utilizing hydroxyl radicals ($^{\bullet}OH$) as the oxidant has been intensively investigated in the past decades [5–7]. As one of the most popular AOPs, Fenton reaction has been successfully adopted in various organic pollutants control and recalcitrant compounds degradation [8–14]. However, the required acidic condition is the major drawback for Fenton reactions because of the inevitable neutralization process and secondary sludge pollution generation [10,15–17]. Therefore, lots of research efforts have been invested into development of effective heterogeneous Fenton catalysts suitable for mild conditions, which could avoid the neutralization process and formation of secondary sludge [18–20]. Various heterogeneous Fenton catalysts including carbon nanotube-supported Fe_3O_4, nanometer zero valent iron, and metal doped iron oxide have been reported [13,21–28]. However, these efficient catalysts processing are complicated and expensive, which is not suitable for large-scale applications.

In this report, the low cost mechanochemical method is adopted to fabricate micron size $FeS_{1.92}$ as heterogeneous Fenton catalysts. The mechanochemical approach exhibits technical advantages of small particle sizes and low agglomeration besides its low cost for large-scale fabrications [29–32]. Specifically, the synthesis of a stable sulfured microscale $FeS_{1.92}$ by ball milling mackinawite (FeS) with sulfur powder (S) is demonstrated in this work. Mechanochemically fabricated $FeS_{1.92}$ shows high catalytic activities for heterogeneous Fenton reaction under mild condition. Furthermore, this $FeS_{1.92}$ Fenton catalyst also shows high sulfide resistance and low Fe^{3+} leaching.

In mechanical milling synthesis, FeS and S powders were mixed together by different ratios. The ball milling process with intensive fracturing and grinding would promote the solid state reaction of FeS with sulfur, which lead to the formation of $FeS_{1.92}$ alloy phase [33,34]. The X-ray diffraction (XRD) pattern of as synthesized sample (Fig. 1a) shows the peaks related to FeS, S and $FeS_{1.92}$. The peak intensity of S becomes stronger with increasing the molar ratios of S/FeS (Fig. S1 in Supporting information). This XRD results suggest that the mechanochemical synthesis can obtain the $FeS_{1.92}$ with some FeS and S remained. In order to verify the chemical structures of $FeS_{1.92}$, we then washed the sample with CS_2 to remove the free sulfur. The XRD peaks of washed $FeS_{1.92}$ exhibit characteristic $FeS_{1.92}$ peaks. The scanning electron microscope (SEM) image of $FeS_{1.92}$ sample shows a floccus morphology, which is related to the mixture of free S with FeS (Fig. 1b and Fig. S2 in Supporting information). The elemental mapping shows that the main element components of the as-synthesized catalyst are Fe and S, which are homogeneously distributed (Fig. S3 and Table S2

* Corresponding author.
E-mail address: yixin.zhao@sjtu.edu.cn (Y. Zhao).

https://doi.org/10.1016/j.cclet.2019.11.049
1001-8417/

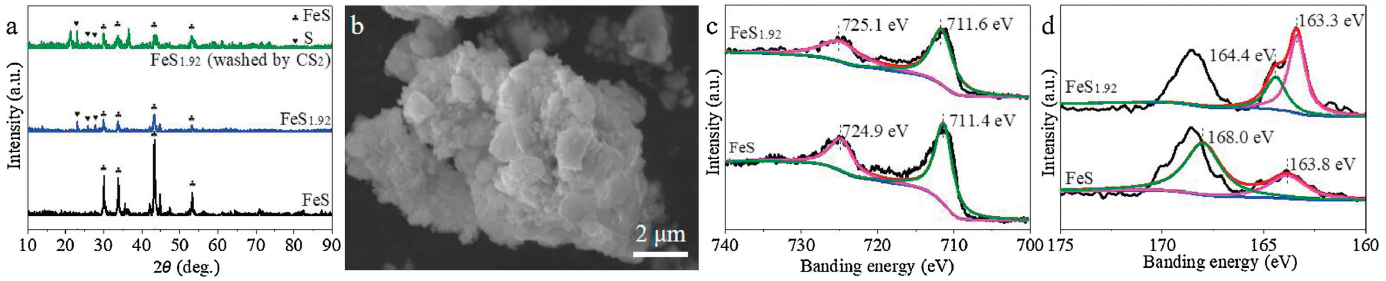

Fig. 1. (a) XRD patterns of FeS raw material and obtained $FeS_{1.92}$ powder before and after washed by CS_2. (b) SEM image of $FeS_{1.92}$. (c) Fe 2p XPS spectra of FeS and $FeS_{1.92}$. (d) S 2p XPS spectra of FeS and $FeS_{1.92}$.

in Supporting information). The energy dispersive X ray spectroscopy (EDS) measurement suggests the S content in $FeS_{1.92}$ is about twice than FeS (Table S3 in Supporting information). X-ray photoelectron spectroscopy (XPS) measurement was performed to explore the chemical bond information of the Fe and S. Two main peaks of FeS sample locate at 724.9 eV and 711.4 eV, which can be assigned to $2p_{1/2}$ and $2p_{3/2}$ of Fe. After sulfuring treatment, these two main peaks shift to the higher banding energy (725.1 eV and 711.6 eV) (Fig. 1c). In contrast, $FeS_{1.92}$ has two 163.3 eV and 164.4 eV peaks related to S^{2-} and S^0 in Fig. 1d. All these results confirm the reaction between FeS and S during the ball-milling process.

The catalytic activation of H_2O_2 by $FeS_{1.92}$ catalyst was tested in the simulated sulfide-containing organic wastewater, which was prepared by adding Na_2S in Bisphenol A (BPA) solution under mild conditions. Fig. 2a showed the catalytic activation of H_2O_2 using different catalysts with or without [Na_2S]. Neither $FeS_{1.92}$ nor H_2O_2 alone showed any activites for BPA degradation. The regular Fenton system (Fe^{2+}/H_2O_2) can remove nearly 60% of BPA in the absent of [Na_2S]. However, its removal efficiency decreased to only 10% in the presence of [Na_2S] because the Fe^{2+} would be deactivated by S^{2-}. Excitingly, the $FeS_{1.92}/H_2O_2$ system exhibited excellent BPA degradation activities with or without [Na_2S]. The catalyst of FeS and S, which was prepared by regular mixing and grinding of the same S/FeS molar ratio, did not present the same catalytic performance. Thus, it can be speculated that the alloy of FeS and S was formed by ball-milling, which is important for the heterogeneous Fenton reaction in sulfide-containing organic pollutants water.

In order to optimize the S/FeS molar ratio for FeS_x catalysts, we studied the catalytic activities of several FeS_x catalysts with different S/FeS molar ratios. Fig. 2b shows the $FeS_{1.92}$ show the highest Fenton catalytic performance. It seems that the added S can increase the active sites on the surface of FeS to activate H_2O_2 to produce $^{\bullet}OH$ for a better catalytic capacity. When the S powder was insufficient, the catalyst exhibited lower activities. However, too much S would reduce the catalytic activities because too much S

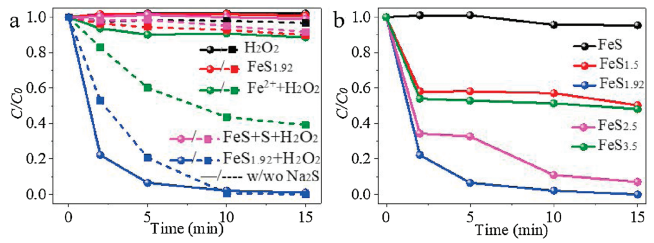

Fig. 2. (a) Degradation rates of BPA with $FeS_{1.92}$ and control experiments. (b). Degradation rates of BPA over several catalysts with different S/FeS molar ratios. Reaction conditions: [catalyst] = 0.25 g/L, [H_2O_2] = 7.5 mmol/L, [BPA] = 100 mg/L, [Na_2S] = 0.2 g/L, pH 6.0.

will cover the active sites on the surface. The $FeS_{1.92}$ could be the optimal for FeS_x based heterogeneous Fenton catalysts. The pH value and H_2O_2 concentration have great impact on the Fenton performance of $FeS_{1.92}$. The degradation efficiency decrease with increase of pH values. The BPA can hardly be oxidized or decomposed when pH values are 8 and 10, which was attributed to the formation of iron hydroxide coating on the catalyst surface and the rapid self-decomposition of H_2O_2 under alkaline conditions [35,36]. However, Fig. S4 (Supporting information) shows that a larger amount of Fe^{3+} leaching was observed under lower pH conditions. The pH 6–7 is the optimal condition to suppress Fe leaching and keep catalytic activity of $FeS_{1.92}$ (Fig. 3a). Here we selected the pH 6 for the heterogeneous $FeS_{1.92}$ performance evaluation. When the H_2O_2 concentration increases from 2.5 mmol/L to 7.5 mmol/L, the degradation efficiency slightly increases (Fig. 3b). Therefore, the H_2O_2 concentration was maintained at 7.5 mmol/L. Moreover, the S^{2-} concentration in wastewater also affects the degradation performance of $FeS_{1.92}$. Interestingly, the $FeS_{1.92}$ showed enhanced catalytic activities for BPA degradation when the S^{2-} concentration reached up to 0.8 g/L (Fig. 3c). Such enhancement might be ascribed to that the more Fe active sites could formed on the $FeS_{1.92}$ surface under the S^{2-}-rich condition because the S_n^{2-} accumulated on $FeS_{1.92}$ surface can promote the reduction of Fe^{3+} to Fe^{2+} [37]. When the concentration of S^{2-} increased up to 1.2 g/L, it began to inhibit the degradation of BPA and it is due to that the $^{\bullet}OH$ radicals can react with the redundant S^{2-}, resulting in the inhibition of BPA degradation.

The stability of $FeS_{1.92}$ was also evaluated under the optimal condition with pH 6.0, 7.5 mmol/L H_2O_2 and 0.2 g/L Na_2S. After four cycles, the $FeS_{1.92}$ still showed excellent degradation performance and an even better catalytic activity (Fig. 3d). During the cycle experiment, the S^{2-} can be accumulated on $FeS_{1.92}$ surface, which can promote the Fe^{3+}/Fe^{2+} cycle and then enhance the performance for the degradation of BPA. Additionally, the Fe^{3+} concentration in the solution after reaction was below 1.0 ppm in the repeated tests (Fig. S5 in Supporting information). No obvious morphology changes can be found in the $FeS_{1.92}$ after reaction as shown in SEM image (Fig. S6 in Supporting information). No change is obviously observed in XRD patterns of $FeS_{1.92}$ before and after the reactions (Fig. S7 in Supporting information), indicating a high chemical stability of $FeS_{1.92}$. Raman spectroscopy also showed no significant changes on $FeS_{1.92}$ surface before and after the reaction (Fig. S8 in Supporting information). However, the XPS of $FeS_{1.92}$ before and after the reaction showed that the proportion of S in $FeS_{1.92}$ decreased. This is probably because S in $FeS_{1.92}$ was consumed as a sacrificial agent during the reactions (Fig. 4a and Fig. S9 in Supporting information). These results show that $FeS_{1.92}$ is a promising catalyst for degradation of sulfide-containing organic pollutants water in heterogeneous Fenton system. We further evaluated the removal efficiency of two more organic pollutants including 2,4,6-trichlorophenol (TCP) and sodium benzene

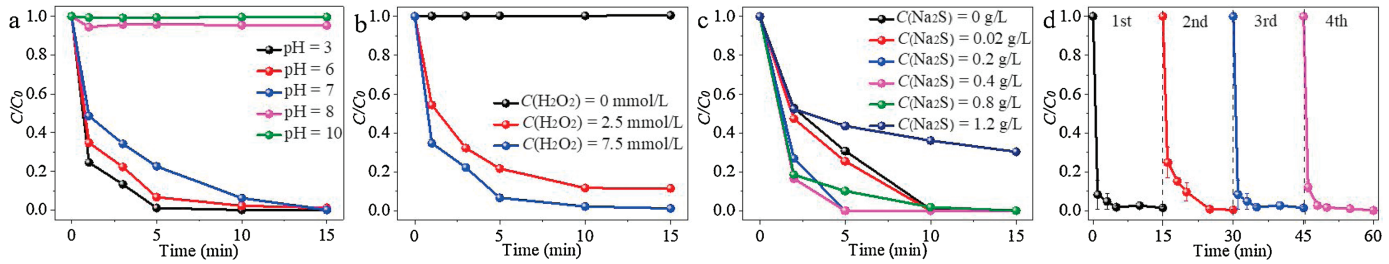

Fig. 3. Effects of pH values (a), H_2O_2 concentrations (b), Na_2S concentrations (c) on BPA removal efficiency. Cyclic stability of $FeS_{1.92}/H_2O_2$ system for BPA degradation (d). Reaction conditions: [catalyst] = 0.25 g/L, [BPA] = 100 mg/L, [H_2O_2] = 7.5 mmol/L for a, c and d, [Na_2S] = 0.2 g/L for a, b and d, pH 6.0 for b, c and d.

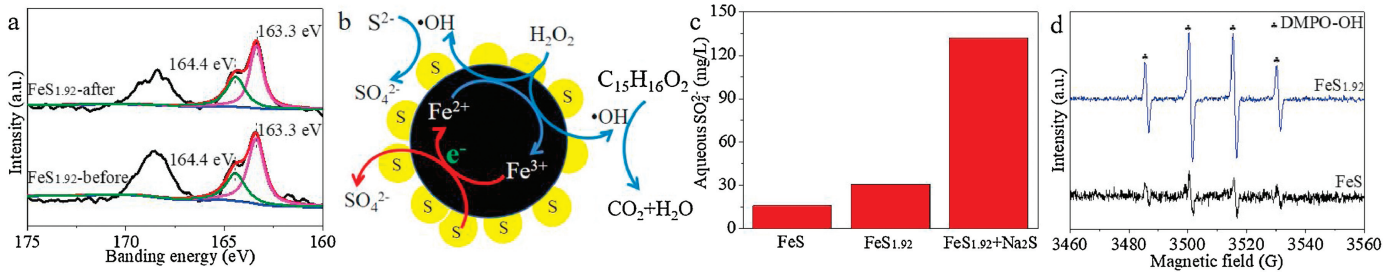

Fig. 4. (a) The proposed scheme of H_2O_2 activation by $FeS_{1.92}$. (b) S 2p XPS spectra of $FeS_{1.92}$ before and after reaction. (c) The concentration of SO_4^{2-} in the solution after the reaction. (d) 5,5-Dimethyl-1-pyrroline *N*-oxide (DMPO) spin capture EPR spectrum in different reaction systems. Reaction conditions: [catalyst] = 0.25 g/L, [H_2O_2] = 7.5 mmol/L, [BPA] = 100 mg/L, pH 6.0.

sulfonate (SBS). We can see that both TCP and SBS pollutants are completely degraded within 15 min, and their mineralization efficiency was relatively high (Figs. S10 and S11 in Supporting information).

The degradation mechanism of organic compounds in $FeS_{1.92}/H_2O_2$ system was investigated. As shown in Fig. 4b, the Fe^{2+} as the active sites in $FeS_{1.92}$ was easily oxidized to Fe^{3+}, inducing the formation of the $^{\bullet}OH$ radicals (Eq. 1) [38–41]. Then, the $^{\bullet}OH$ radicals can mineralize organic pollutants into CO_2 and H_2O. The S^0 or S_n^{2-} on $FeS_{1.92}$ surface, as the electron donor, can react with Fe^{3+} to form Fe^{2+} and improve the Fe^{3+}/Fe^{2+} cycle (Eqs. 2 and 3) [42–44]. Compared with FeS, the chemical bonding between FeS and S in $FeS_{1.92}$ can promote the Fe^{3+}/Fe^{2+} cycle for better degradation performance. When the solution contains appropriate amount of S^{2-}, it can also promote the conversion of Fe^{3+} to Fe^{2+} (Eq. 4) [37].

$$Fe^{2+} + H_2O_2 \rightarrow Fe^{3+} + OH^- + {}^{\bullet}OH \quad (1)$$

$$S + 6Fe^{3+}\ 4H_2O \rightarrow 6Fe^{2+}\ SO_4^{2-} + 8H^+ \quad (2)$$

$$Sn^{2-} + (6n + 2)Fe^{3+} + 4nH_2O \rightarrow (6n + 2)Fe^{2+} + nSO_4^{2-} + 8nH^+ \quad (3)$$

$$8Fe^{3+} + S^{2-} + 4H_2O \rightarrow 8Fe^{2+} + SO_4^{2-} + 8H^+ \quad (4)$$

To verify this speculation, the evolution of surface S in $FeS_{1.92}$ during Fenton reaction was investigated. According to the XPS analysis, the proportion of S_0 or S_n^{2-} in $FeS_{1.92}$ after the reaction decreased, indicating that S was consumed to some extent in the process of the reaction (Fig. 4a and Table S3 in Supporting information). The sulfur seems to be oxidized into SO_4^{2-} and can be detected in the final reaction solution (Fig. 4c). Moreover, the SO_4^{2-} produced in $FeS_{1.92}/H_2O_2$ system is about twice as that produced in FeS/H_2O_2 system, indicating that sulfur added to FeS by ball-milling does participate in the reaction. For a better insight into the role of S in this $FeS_{1.92}$ Fenton catalyst, the effect of SO_4^{2-} in the Fenton reaction was investigated. The result indicated that the SO_4^{2-} did not impact the BPA degradation in $FeS_{1.92}/H_2O_2$ system. This result confirmed that the performance enhancement was mainly attributed to the formation of S^0 or S_n^{2-} on $FeS_{1.92}$ surface (Fig. S12 in Supporting information). Electron paramagnetic resonance (EPR) analysis was also conducted to explore the above mechanism. As shown in Fig. 4d, the hydroxyl radical adducts of 5,5-dimethyl-1-pyrroline *N*-oxide (DMPO-OH) (1:2:2:1) signal was observed in $FeS_{1.92}/H_2O_2$ system, indicating the generation of $^{\bullet}OH$ radicals in the sulfide-containing solution. The relative EPR intensity of $FeS_{1.92}/H_2O_2$ system exhibit higher EPR intensity than that of FeS/H_2O_2 system. These results indicated that S in $FeS_{1.92}$ promote the $^{\bullet}OH$ radicals generation especially in the sulfide-containing organic pollutants water.

In summary, a highly efficient $FeS_{1.92}$ based heterogeneous Fenton catalyst was synthesized by a facile ball milling of FeS with S powder. In the mechanochemical reaction, the S species can reduce Fe^{3+} to Fe^{2+} for Fenton-like reaction. At the same time, this $FeS_{1.92}$ Fenton catalyst shows a highly sulfide resistance and improved performance for degrading sulfide-containing organic pollutants. This work has broadened the application of FeS_x based environmental catalyst in wastewater treatment, especially for sulfide-containing organic pollutants water.

Declaration of competing interest

The authors declare that they have no known competing financial interests or personal relationships that could have appeared to influence the work reported in this paper.

Acknowledgments

This work was supported by the National Natural Science Foundation of China (No. 21777097) and Shanghai Shuguang Grant

(No. 17SG11) and the China Postdoctoral Science Foundation (Nos. 2017M621483, 2018T110397).

Appendix A. Supplementary data

Supplementary material related to this article can be found, in the online version, at doi:https://doi.org/10.1016/j.cclet.2019.11.049.

References

[1] I. Ali, M. Asim, T.A. Khan, J. Environ. Manag. 113 (2012) 170–183.
[2] T. Deblonde, C. Cossu-Leguille, P. Hartemann, Int. J. Hyg. Environ. Health 214 (2011) 442–448.
[3] R. Rosal, A. Rodriguez, J.A. Perdigon-Melon, et al., Water Res. 44 (2010) 578–588.
[4] J. Xiao, Y. Xie, H. Cao, Chemosphere 121 (2015) 1–17.
[5] T. An, H. Yang, G. Li, et al., Appl. Catal. B: Environ. 94 (2010) 288–294.
[6] Y. Deng, R. Zhao, Curr. Pollut. Rep. 1 (2015) 167–176.
[7] K.E. O'Shea, D.D. Dionysiou, J. Phys. Chem. Lett. 3 (2012) 2112–2113.
[8] A. Babuponnusami, K. Muthukumar, J. Environ. Chem. Eng. 2 (2014) 557–572.
[9] S. Giannakis, M.I. Polo López, D. Spuhler, et al., Appl. Catal. B: Environ. 199 (2016) 199–223.
[10] E. Neyens, J. Baeyens, J. Hazard. Mater. 98 (2003) 33–50.
[11] M.C. Pereira, L.C.A. Oliveira, E. Murad, Clay Miner. 47 (2018) 285–302.
[12] J.J. Pignatello, E. Oliveros, A. MacKay, Crit. Rev. Environ. Sci. Technol. 36 (2006) 1–84.
[13] S. Rahim Pouran, A.A. Abdul Raman, W.M.A. Wan Daud, J. Clean. Prod. 64 (2014) 24–35.
[14] M. Umar, H.A. Aziz, M.S. Yusoff, Waste Manag. 30 (2010) 2113–2121.
[15] A.D. Bokare, W. Choi, J. Hazard. Mater. 275 (2014) 121–135.
[16] J. Kochany, E. Lipczynska-Kochany, J. Hazard. Mater. 166 (2009) 248–254.
[17] A. Mirzaei, Z. Chen, F. Haghighat, L. Yerushalmi, Chemosphere 174 (2017) 665–688.
[18] P.V. Nidheesh, RSC Adv. 5 (2015) 40552–40577.
[19] X. Qian, M. Ren, Y. Zhu, et al., Environ. Sci. Technol. 51 (2017) 3993–4000.
[20] G. Zhang, S. Wang, F. Yang, J. Phys. Chem. C 116 (2012) 3623–3634.
[21] V. Cleveland, J.P. Bingham, E. Kan, Sep. Purif. Technol. 133 (2014) 388–395.
[22] R.A. Crane, T.B. Scott, J. Hazard. Mater. 211-212 (2012) 112–125.
[23] J. Deng, X. Wen, Q. Wang, Mater. Res. Bull. 47 (2012) 3369–3376.
[24] I.R. Guimaraes, A. Giroto, L.C.A. Oliveira, et al., Appl. Cata. B: Environ. 91 (2009) 581–586.
[25] B.H. Moon, Y.B. Park, K.H. Park, Desalination 268 (2011) 249–252.
[26] T. Soltani, A. Tayyebi, B.K. Lee, Appl. Surface Sci. 441 (2018) 853–861.
[27] Y. Wang, H. Zhao, G. Zhao, Appl. Catal. B: Environ. 164 (2015) 396–406.
[28] S. Zha, Y. Cheng, Y. Gao, et al., Chem. Eng. J. 255 (2014) 141–148.
[29] L.C. Damonte, M.A. Hernández-Fenollosa, B. Marí, J. Alloys. Compd. 434-435 (2007) 813–815.
[30] C. Mochales, R.M. Wilson, S.E.P. Dowker, M.P. Ginebra, J. Alloys. Compd. 509 (2011) 7389–7394.
[31] B. Nasiri-Tabrizi, P. Honarmandi, R. Ebrahimi-Kahrizsangi, P. Honarmandi, Mater. Lett. 63 (2009) 543–546.
[32] A. Tadjarodi, M. Imani, Mater. Lett. 65 (2011) 1025–1027.
[33] P.P. Chin, J. Ding, J.B. Yi, B.H. Liu, J. Alloys. Compd. 390 (2005) 255–260.
[34] C.K. Lin, C.L. Du, G.S. Chen, et al., Mater. Sci. Eng. A 375–377 (2004) 834–838.
[35] Y.S. Jung, W.T. Lim, J.Y. Park, Y.H. Kim, Environ. Technol. 30 (2009) 183–190.
[36] K. Toda, T. Tanaka, Y. Tsuda, et al., J. Hazard. Mater. 278 (2014) 426–432.
[37] L. Zhao, Y. Chen, Y. Liu, C. Luo, D. Wu, Chemosphere 188 (2017) 557–566.
[38] R. Gonzalez-Olmos, F. Holzer, F.D. Kopinke, A. Georgi, Appl. Catal. A: Gen. 398 (2011) 44–53.
[39] L. Xu, J. Wang, J. Hazard. Mater. 186 (2011) 256–264.
[40] L. Xu, J. Wang, Appl. Catal. B: Environ. 123–124 (2012) 117–126.
[41] T. Zhou, Y. Li, J. Ji, F.S. Wong, X. Lu, Sep. Purif. Technol. 62 (2008) 551–558.
[42] J. Fan, L. Gu, D. Wu, Z. Liu, Chem. Eng. J. 333 (2018) 657–664.
[43] S. Guo, Z. Yang, Z. Wen, et al., J. Colloid Interface Sci. 532 (2018) 441–448.
[44] Y. Zhou, X. Wang, C. Zhu, et al., Water Res. 142 (2018) 208–216.